International Journal of Impact Engineering 000 (2017) 1–9

Contents lists available at ScienceDirect

International Journal of Impact Engineering

journal homepage: www.elsevier.com/locate/ijimpeng

# Experimental and numerical studies on the failure modes of steel cabin structure subjected to internal blast loading

Shujian Yao*, Duo Zhang*, Fangyun Lu, Xiangcheng Li

*College of Science, National University of Defense Technology, Changsha, Hunan 410073, PR China*

ARTICLE INFO

*Article History:*

*Keywords:*
Internal blast
Failure modes
Failure process
Steel cabin
Experiment study

ABSTRACT

Two series of experiments were conducted with different dimension and different masses of explosive. The failure processes of the side plate were recorded by using high-speed photography system. Damage features of the experimental results were analyzed. The results show that the damage degree increases with the increasing of TNT mass. In larger TNT mass cases, cracks produce in both the edge and the central of side plate, and some plates may eject out with relatively high launch velocity which are destructive to the adjacent cabins. During the deformation process, the edge and corner area of side plate may produce large deformation due to the intensified internal shock waves which is different from external explosion.

Meanwhile, a number of numerical simulations were carried out by using the validated numerical method. Through analyzing the numerical and experimental results, three damage forms of cross-shaped damage, curve-shaped damage and sphere-shaped were observed. In cross-shaped damage form, six failure modes were concluded: plastic deformation (mode I); petalling in plates center (mode $II^*_C$); Capping in plates center (mode $II_C$); corner shear failure (mode $III_{in}$); edge tearing (mode II); and shear failure over entire plate (mode III). In addition, the failure process and mechanisms of each mode were also analyzed.



## 1. Introduction

Research into failure modes has long been a focus of attention for researchers, because different failure modes correspond to different mechanisms. Menkes and Opat [1] proposed three failure modes for a clamped beam subjected to uniformly distributed loads in 1971: mode I (large inelastic deformation); mode II (tensile failure at the support); and mode III (transverse shear failure at the support). Experiment studies [2–7] and numerical simulations [8,9] showed that these three failure modes happened in turn with increasing uniformly distributed impulsive loads. Studies on plates subjected to localised blast [10–13] showed that the failure modes of large inelastic deformation and tensile failure at the support were also observed, but transverse shear failure did not occur. Jacob et al. [14] summarized the failure modes of plate subjected to localized blast loading, pointing out that there were other failure modes (necking, capping, and petalling [13,15]) produced in the loaded area of the plate which arose with increasing impulsive load. Research has showed that the shape and magnitude of pulse pressure [16,17], mass of explosive [18,19], explosive distance [7,14] and the boundary conditions [11,20–22] had significant effects on the failure modes. Nurick and Shave [20] notes that there is a critical impulsive load between two neighbouring failure modes and sometimes the same impulsive load corresponds to a different failure mode if it is applied at a different loading position and with different boundary conditions.

Multi-steel-cabin structures are common in ships and steel box girders in large bridges. The ships and large box-girder bridges are facing the threat of internal explosion for many reasons, such as occasional explosion, terrorism attack and military strike. In military strike, with the purpose of destroying the facility and attacking the crew inside the ship, advanced missile with time-delay fuse was used which was designed to detonate after penetrating the deck or side plate.

Internal explosions are complicated and that they are more destructive than normal explosions [23–25]. Existing research related to internal explosions in cabin structure is rare. Hu and Zhao [26] studied the magnitude and distribution of internal explosion loading on large-scale cylindrical tanks with fixed roof through numerical simulations. Dong et al. [27] studied the interactive mechanisms between internal blast loading and the dynamic elastic response of spherical containment vessels. Ma et al. [28] studied containment vessels subjected to internal blast loading and analyzed the different modes of both ductile and brittle failures. Geretto et al. [29] performed a series experiments of square mild steel plates subjected to blast loads in three different degrees of confinement and

* Corresponding authors.
*E-mail address:* yaoshujian@gmail.com (S. Yao), duo.w.zhang@gmail.com (D. Zhang).

http://dx.doi.org/10.1016/j.ijimpeng.2017.03.006
0734-743X/© 2017 Published by Elsevier Ltd.

investigated the effects of confinement as well as the effect of plate thickness on the final plate deformations.

The present work focus on analyzing the failure modes of steel cabin structure under internal blast loading. Two series of experiments with different dimension and explosive mass were set-up and the damage features as well as failure processes were obtained. Then numerical method was introduced and a number of simulations were conducted. Based on the experimental and numerical results, the failure modes and mechanism were concluded and discussed.

## 2. Experiment studies

Full-scale experiments involving actual geometries and charges are complicated and costly in terms of both preparation and measurements. Thus, scaled-down experiments are highly desirable. In the current research, two series of steel cabin models, names single cabin model (SC) and multi-cabins model (MC), with different explosive charge are designed to investigate the failure modes of cabins under internal blast loading.

### 2.1. Experiment setup

Fig. 1 shows the design details and manufactured specimen of the single cabin model. The side length ($L$) of the cuboid specimens is 450 mm and the thickness of all side plates are 3 mm. An extra length of $L/5$ is welded to each plate for the purpose of modeling the boundary condition as real as possible, the whole dimension of this model is 630 mm × 630 mm × 630 mm (as shown in Fig. 1). A hole is reserved in the center of top plate for the purpose of placing the explosive.

Fig. 2 shows the details of the three cabins model. Each cabin of the three cabins model share a same dimension of 0.5 m × 0.5m × 0.5 m, and there is a pressure relief hole between the right side cabin and the middle cabin. The thicknesses of the plates are all 2 mm. The real boundary condition of three cabins model is neither fixed nor simply supported, in fact, the considered cabins of the specimen is connected to other cabins in all directions in the real structure. In the current model, the boundary condition is considered by extending an extra 0.2 m length of each plate (exclude the front side plates) for the purpose of modeling the boundary condition as real as possible. Therefore, the whole dimension of the specimen is 1.9m × 0.7m × 0.9 m (as shown in Fig. 2). The specimen is fixed on the ground by using 6 rivets as shown in Fig. 2.

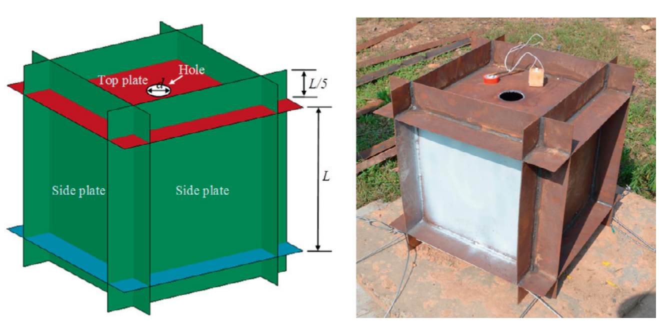


(a) Design details (b) Test specimen

**Fig. 1.** The single cabin model.

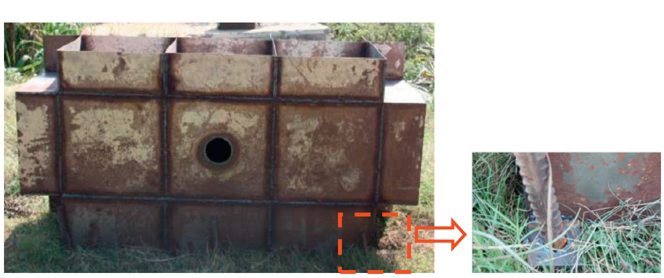

**Fig. 2.** The three cabins model.

**Table 1.**
Mechanical properties of Q235B steel plate.

| Plate thickness (mm) | Yield strength (MPa) | Ultimate tensile strength (MPa) | Young's modulus (GPa) | Percentage elongation (%) |
|---|---|---|---|---|
| 2mm | 370 | 485 | 200 | 30 |
| 3mm | 368 | 484 | 200 | 29 |

The single cabin models and the three cabins models are made up of 3 mm thickness and 2 mm thickness Q235B steel plates, respectively. These specimens are all manufactured through both sides fillet welding. The Mechanical properties of Q235B steel plate are given in Table 1. In which the yield strengths of 2 mm and 3 mm thickness plate are 370 MPa and 368 MPa, respectively.

High-speed photography system is applied here with expectation of observing the failure process. High-speed camera was protected by a steel box shield as shown in Fig. 3. In addition, to protect the camera lens, a mirror was used to transfer the test images. The test specimen is placed at about 3 m away from the mirror along the direction of incidence image.

### 2.2. Experimental cases

TNT explosive with a density of 1.5 g/cm$^3$ is used in the present study for it is a standard high explosive which is chemically safe and easy to cast. The TNT explosive is suspended in the center of the central cabin and ignited by an electronic detonator which is inserted into the top of the TNT. Four tests with different TNT mass of 40.5 g to 231.55 g are designed for single cabin test, named as SC-1 ∼ SC-4. Meanwhile, two cases (TC-1 and TC-2) for three cabins models are designed. Hence, there are totally six tests, the details of experiment cases are listed in Table 2, in which the scaled distance $Z = R/W^{(1/3)}$, where $W$ is TNT mass and $R = L/2$ is the distance between the explosive position and the side plate of the central cabin.

### 2.3. Experimental results analysis

Fig. 4 shows the experimental results of the single cabin tests. The results show that the damage degree increases with the increasing of TNT mass. Outward bulging of the whole plate is observed in all sides of tests SC-1, SC-2 and SC-3, and inplane buckling produces

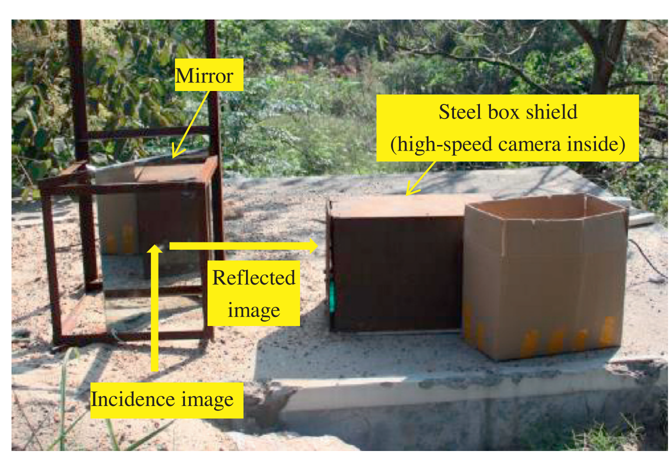


**Fig. 3.** High-speed photography system.

Please cite this article as: S. Yao et al., Experimental and numerical studies on the failure modes of steel cabin structure subjected to internal blast loading, International Journal of Impact Engineering (2017), http://dx.doi.org/10.1016/j.ijimpeng.2017.03.006